

Effect of Copper Content on Corrosion Resistance of Dental Amalgam

Dr. Haydar H. J. Jamal Al-Deen*[#], Dr. Ali Hubi Haleem* & Mohammad Saad Tuma**

* Asst. Professor, Dept. of Metallurgical Engineering, Materials Engineering College, University of Babylon, Babylon, Iraq.

**Materials Engineering, University of Babylon, Babylon, Iraq.

jaberjd@gmail.com.

Article Info

Volume 83

Page Number: 24203 – 24216

Publication Issue:

May - June 2020

Abstract

The fundamental objective of this research is to explore the impact of copper content on corrosion resistance of dental amalgam. Five alloys have been casted made out of steady level of tin (30wt %) and the copper content is fluctuate from 5 to 25wt% with interim of 5%. Copper is increased in the expense of silver. The specimens were prepared according to ADA specification No. 1 and have been stored at 37 ± 1 °C. The corrosion test has been carried out according to ASTM standard (G5 – 87) and at 37 ± 1 °C. Two types of electrochemical tests were made an Open Circuit Potential (OCP) – time measurements, and Potentiodynamic polarization in artificial saliva at 37 ± 1 °C. From the obtained results, it's obvious that the E_{corr} is shifted to the positive side and a reduction in the mean corrosion current densities with copper content increasing, hence, increasing corrosion resistance with increasing copper content by 46 % compared to low copper dental amalgam.

Keywords: dental Amalgam, corrosion, copper content, potentiodynamic test, dental material, artificial saliva

Article History

Article Received: 11 May 2020

Revised: 19 May 2020

Accepted: 29 May 2020

Publication: 12 June 2020

1. INTRODUCTION

Dental amalgam restorations containing mercury has a long history starting with Chinese in 659 A.D. they were the first users of silver-mercury past [1]. It has been in use since the 1800s, generally with limited known harmful effects on humans [2]. Its estimated that 75% of all tooth restorations are amalgam restoration[3,4]. Dental amalgam is easy of manipulation, low cost, low in creep, high in compressive strength and high wear resistance long-term performance, and experiences minimal dimensional change with time[5,6].

Dental silver amalgam is a polyphase material, and the electrode potential differences between the various phases are substantial. Galvanic corrosion of

the highest electropositive phase (i.e. γ_2) therefore, is guaranteed[7]. The resistance to corrosion of various phases in descending order is as follows [8]:

γ (Ag₃Sn) phase > γ_1 (Ag₂Hg₃) phase > silver-copper eutectic phase > ϵ (Cu₃Sn) phase > η (Cu₆Sn₅) phase > γ_2 (Sn₇Hg) phase

Amalgam filling generally tarnishes and shows discoloration but occasionally corrode too. Tarnished amalgam restoration is unaesthetic and if unattended it may lead to corrosion. Products of corrosion may penetrate The tubules of the dentin and cause discoloration of the whole tooth[9]. A variety of factors can influence the corrosion rate. These include acidity of the contacting medium and temperature, which can both undergo sharp

differences over a brief period of time in the oral cavity, as well as the effective of the amalgam potential [10].

Fathi et al. [11] provided a comparative assessment of the initial corrosion of four brand of high copper dental amalgam and discovered that the highest resistance to corrosion was at 25 wt% copper content. Acciari et al. [12] present that the corrosion potentials most positive for γ_1 , followed by γ and then γ_2 , Reflecting the resistance to corrosion. Majed et al.[13] observed that the corrosion resistance was increased with time Because of stable phases which produced between mercury and other powders in amalgam such as γ_2 and γ_1 , in addition to Ag–Cu and γ phases. There are many studies proposed the replacement of mercury with gallium alloy in dental fills the to overcome the hurdle of mercury[14].

This work aims to Evaluate the effect of copper content on corrosion resistance of dental amalgam.

2. EXPERIMENTAL

2.1. Powder Alloy Preparation

The element of amalgam alloys (Ag, Cu, Sn and Zn) are melted by using electrical furnace under inert atmosphere using argon gas. Five alloys have been casted composed of constant percentage of tin 30% and the copper content is varying from 5 to 25% in a step of 5%. Copper increases in the expense of silver. Zinc is added at a constant weight of 1.2 gm per cast (the weight of each cast is 40g). Casting operation is done in the following sequence. Firstly, silver was placed in the crucible in the furnace with normal atmosphere till melting then copper is added piece by piece. The melt is allowed to be super-heated for ten minutes. After that, zinc was added to scavenge oxygen. The inert atmosphere was made immediately after adding zinc by inserting the argon gas tube in to the crucible then tin is added at once. The final step is pouring the melted alloy into a preheated steel mold. The ingots obtained by casting were heat treated for 4 hours at 400 oC to obtain uniform distribution of the

elements and phases. The prepared cast alloys are then converted into powder. This transformation done by turning and ball mill of ceramic balls and polyethylene jar to obtain a mean particle size of 40 μ m. Finally the powder heat treated to relief the stress at 100oC for three hour under vacuum atmosphere. The chemical composition of the alloys is expressed in **Table 1**.

Table 1 Illustrates the chemical composition analysis of the used alloys.

Alloy	Ag wt%	Cu wt%	Sn wt%	Zn wt%
A	66.79	4.95	24.84	2
B	61.1	9.83	27.4	1.82
C	56.2	15.3	23.72	2.4
D	53.69	19.3	25.63	1.8
E	47.81	23.41	26.6	1.6

2.2. Specimens Preparation

The specimens prepared according to the ADA specification No.1 [1] by trituration of equal amount of alloy powder and mercury for 30 sec by mechanical amalgamator type (ling chen). The dimensions of the specimens are (4 mm in diameter & 8 mm in height). The mixed material was packed by hand into a Teflon mold, has the desired dimensions, resting on a flat surface, using a conventional 2 mm diameter condensing point and then, a compressive stress of 14 MN/m² has applied for 85 seconds, later, after 30 minute the die was opened and the specimen ejected. The specimens stored at 37 \pm 1 °C.

2.3. Microstructure Observation

A specimen was taken from each amalgam alloy and cold mounted using room temperature curing polyester resin. Rough polishing was performed on successively finer grades of emery papers (220, 360,400, 600, 800, 1000, 1200, 1500, and 2000), polishing done with the aid of two particles sizes diamond past as follow: 15 μ m then with 0.25 μ m. The specimens were then washed

thoroughly with distilled water and dried in an air blast, and stored in a desiccator for the minimum time possible before etching.

The polished specimens of amalgam alloys were etched by a chemical etchant (30 vol% nitric acid). Then examined under 400x magnification using optical microscopy. The following solutions have been used to etch amalgam samples **Table 2** [16]:

Table 2 Present the etching solutions.

Solution A	Solution B	"Hypo" rinse
4 gm. $K_2Cr_2O_7$	4 gm. I	$Na_2S_2O_3 \cdot 5H_2O$
1 gm. KI	96 ml. ethyl alcohol	Dissolved in water
water 100 ml. H_2O		

The samples were swabbed for 20-40 seconds with Solution A and washed with water. Then it was lightly swabbed with Solution B for 5-15 seconds, followed with a "hypo" swab-rinse, washed with water, and dried.

Scanning electron micrograph was performed using Inspect S50 (FEI company), Netherlands. The distribution of elements on each amalgam surface was qualitatively and quantitatively analyzed.

2.4. Electrolytic Solution

The electrolyte employed in this investigation was artificial saliva (Fusayama solution) which closely resembles the mineral composition of natural saliva, with composition shown in **Table 2** [17].

Table 2 The chemical composition of the artificial saliva [17].

Compound	g/l
NaCl	0.4
KCl	0.4
$CaCl_2 \cdot 2H_2O$	0.906

$NaH_2PO_4 \cdot 2H_2O$	0.69
$Na_2S \cdot 9H_2O$	0.005
urea	1

2.5. Corrosion Test

Two types of electrochemical tests were made: an Open Circuit Potential (OCP) – time measurements, and Potentiodynamic polarization were used as the techniques for evaluating corrosion parameters for all the tested amalgams. The experimental of open circuit potential is performed in a 400ml capacity glass electrolytic cell. The tests were carried out with the specimens immersed in a solution of artificial saliva. The potential of the working electrode (specimen) is measured with respect to a Standard Calomel Electrode (SCE). A voltmeter is connected between the working electrode and the reference electrode. For each specimen, three hours open circuit potential, E_{OC} , measurement was performed. The first record was taken immediately after immersion then the voltage was monitored for the intended period of test at an interval of five minutes.

Electrochemical experiments were performed in a three-electrode cell containing an electrolyte similar to natural saliva. The counter electrode was a Pt electrode and the reference electrode was SCE and working electrode (amalgam) according to ASTM (G5-87) [18]. **Figure 1** shows a schematic diagram of Potentiodynamic polarization cell.

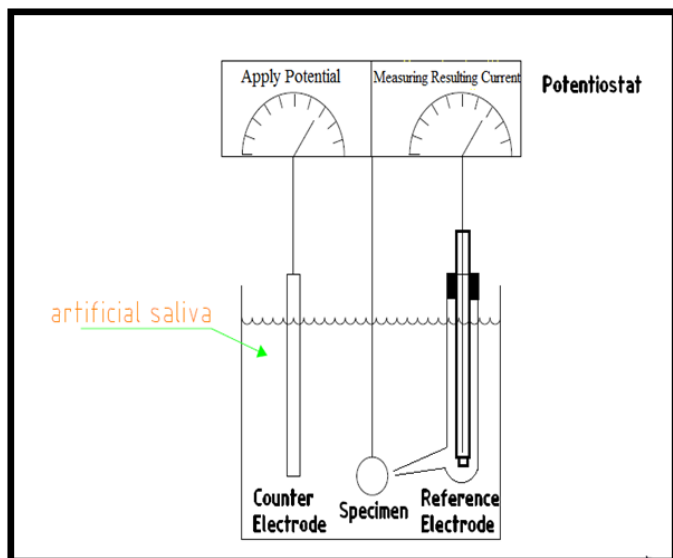


Figure1 Shows a schematic diagram of potentiodynamic polarization cell.

Polarization test were performed in Winking MLab 200. The potentiodynamic polarization curves were plotted and both corrosion current density (i_{corr}) and corrosion potential were estimated by Tafel plots by using both anodic and cathodic branches. The test was conducted by stepping the potential by a scanning rate 0.4 mV/s from an initial potential of 200 mV below the open circuit potential and the scan was continued up to 200 mV above the open circuit potential.

Corrosion rate measurement is obtained by using the equation [19]:

$$\text{Corrosion Rate (mpy)} = 0.13i_{\text{corr}}(E.W) / A.\rho$$

where:

E.W. = equivalent weight (gm/eq.).

A = area (cm^2).

ρ = density (gm/cm^3).

0.13 = metric and time conversion factor.

i_{corr} = current density ($\mu\text{A}/\text{cm}^2$).

3.RESULT AND DISCUSSION

Figure (2-6) shows the microstructure of amalgam alloys before and after homogenization heat treatment. **Figures2(a) -6(a)** are as cast alloys, the crystals which form in the liquid during freezing generally have a configuration consisting of a main branch with many appendages. A crystal of such a morphology is named a dendrite. The dendritic structure is formed during the constitutional supercooling of the casts. The frozen structure consists of dendrites in which the central regions of the main branch and of the sidearms contain less of the alloying element than the regions where the sidearms met on completion of freezing. The chemical gradients in the dendritically cored structure shown were reduced to an acceptable level by homogenization heat treatment.

Figures 2(b) -6(b) shows the microstructure after the homogenization heat treatment. These figures reflect the effectiveness of the performed heat treatment where a more homogenous structure is presented. These structures are consist mainly of two regions; matrix as white region and dark regions. These regions represent γ as the white region and ϵ as the dark regions.

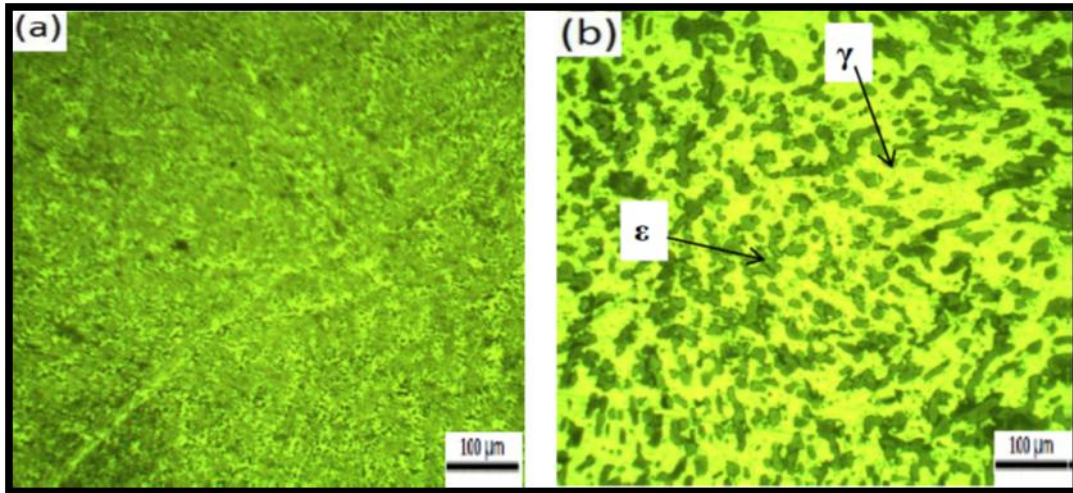


Figure (2) The microstructure of the A amalgam alloy. (a)As cast structure (b) After homogenization heat treatment

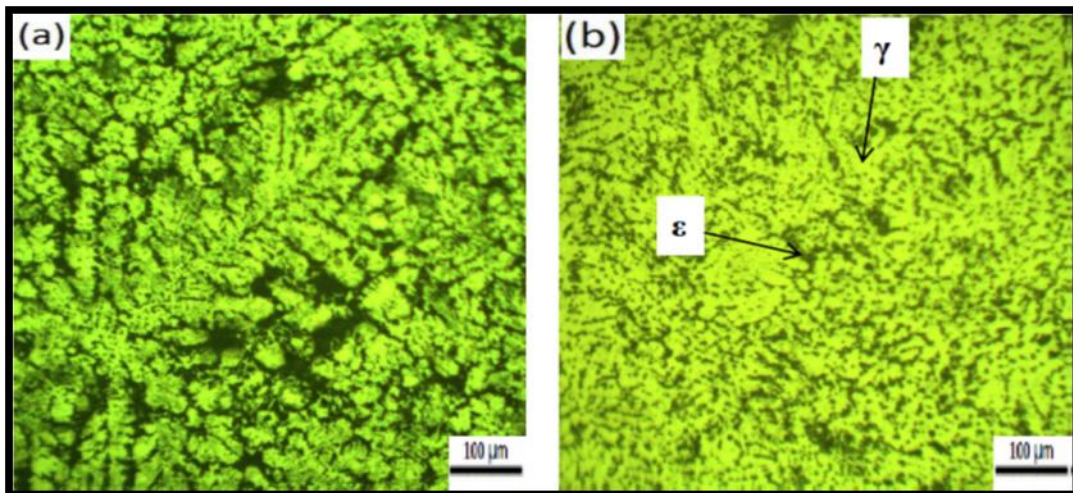


Figure (3) The microstructure of the B amalgam alloy. (a)As cast structure (b) After homogenization heat treatment

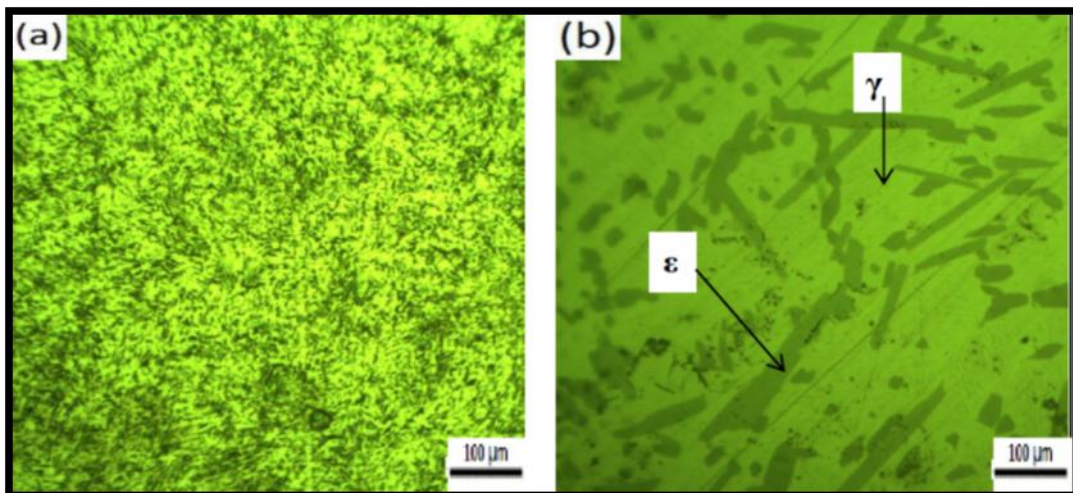


Figure (4) The microstructure of the C amalgam alloy. (a) As cast structure (b) After homogenization heat treatment

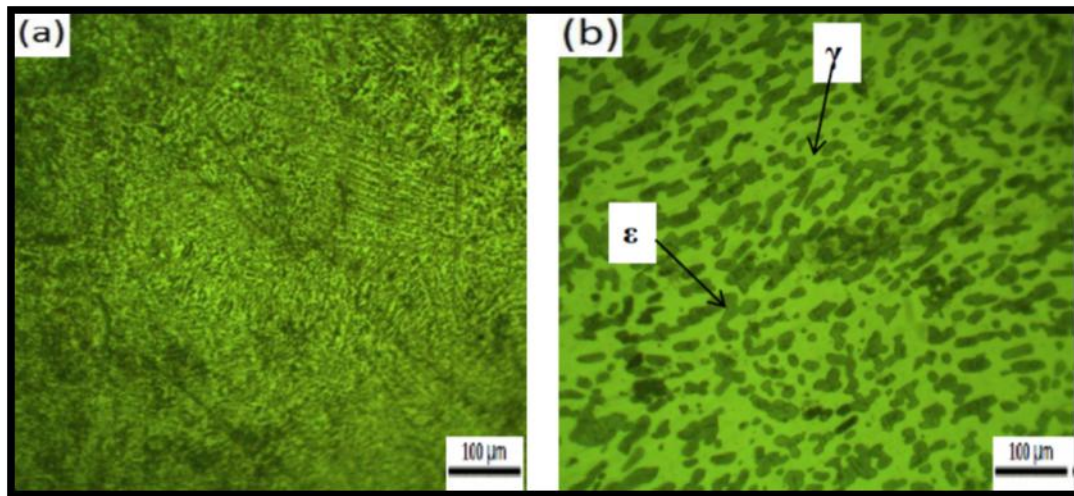


Figure (5) The microstructure of the D amalgam alloy. (a) As cast structure (b) After homogenization heat treatment

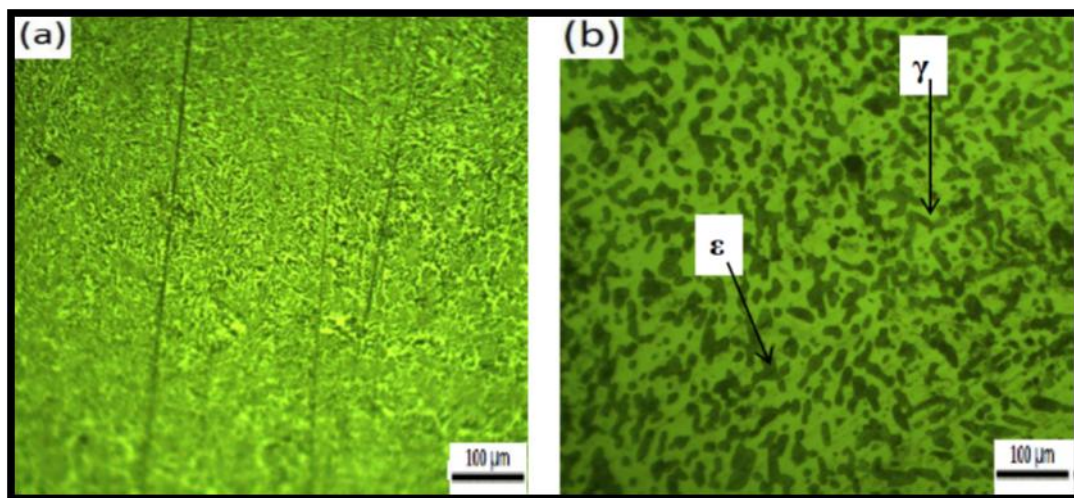


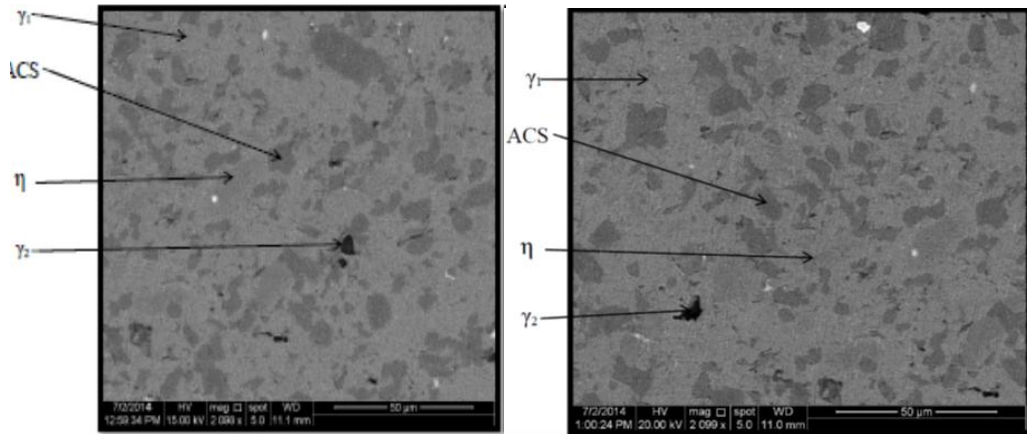
Figure (6) The microstructure of the E amalgam alloy. (a) As cast structure (b) After homogenization heat treatment

SEM equipped with an energy dispersive spectrometer (EDS) was performed and **Figure 7** shows microstructure and **Figure 8** shows the EDS results. Three regions were selected for EDS: First region is the gray particles, this region, in all amalgams, contain the entire alloying element used in amalgam alloys (Ag, Sn, Cu and Zn) in addition to oxygen and Hg. The oxygen found was forming with zinc ZnO as reserved from the EDS result. Presence of minut amount of Hg resulted from the formation

of the electron beam beneath the surface layers of the specimen. With this result these regions are certainly the unreacted particles.

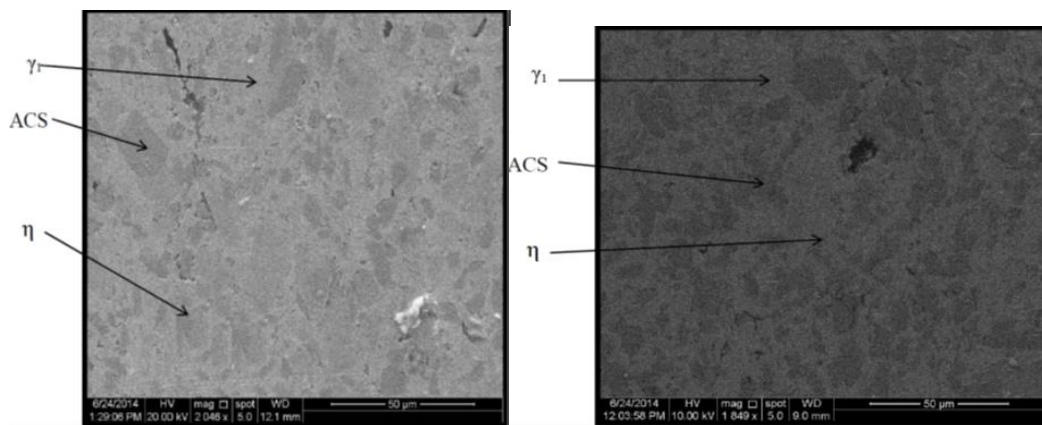
The second region is the light gray (the matrix) the highest element content is Hg and Ag, this is thought to be γ_1 phase. At the same region η phase also found as other spot in the same region a higher content of Cu and Sn was found.

Another phase was found in the A and B rich in Hg and Sn. This phase is γ_2 phase. amalgams and its rare in the black regions which is



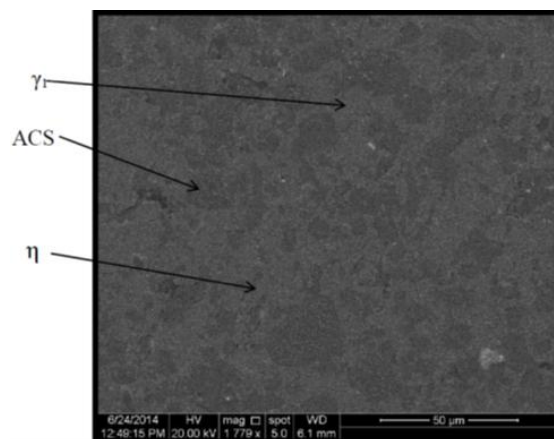
Amalgam (a)

Amalgam (b)



Amalgam (c)

Amalgam (d)



Amalgam (e)

Figure 7 SEM micrograph of the A amalgam.

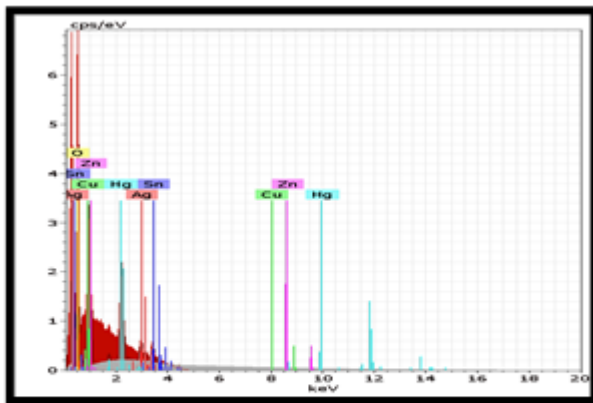


Figure a Shows spectrum of EDS analysis for the first region of amalgam A.

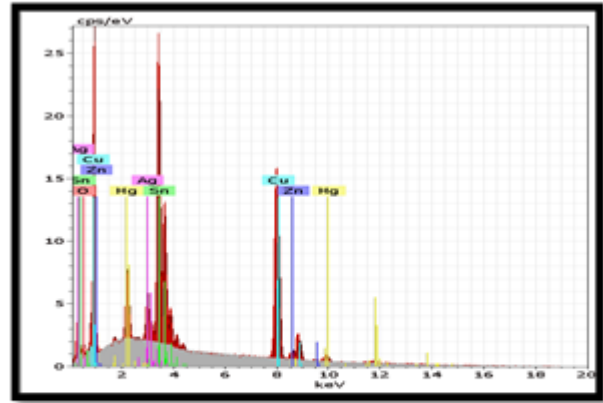


Figure b Shows spectrum of EDS analysis for the second region of amalgam A.

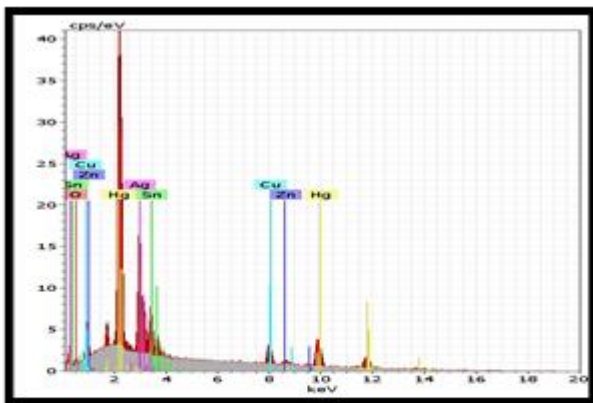


Figure c Shows spectrum of EDS analysis for the third region of amalgam A.

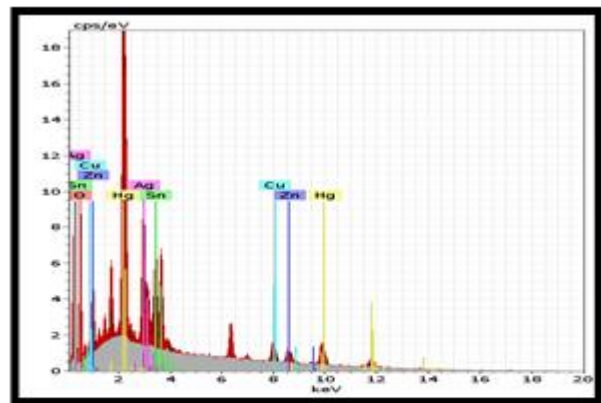


Figure d Shows spectrum of EDS analysis for the fourth region of amalgam A.

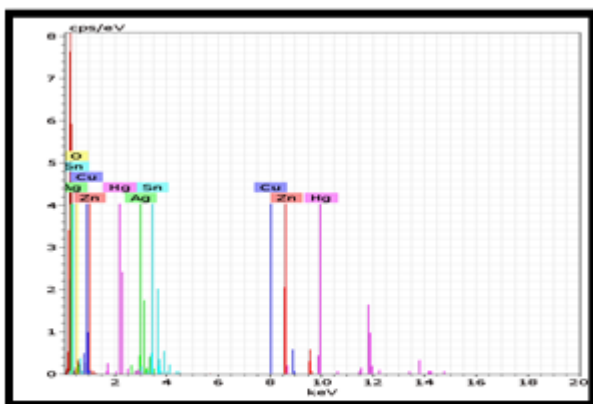


Figure e Shows spectrum of EDS analysis for the first region of amalgam B.

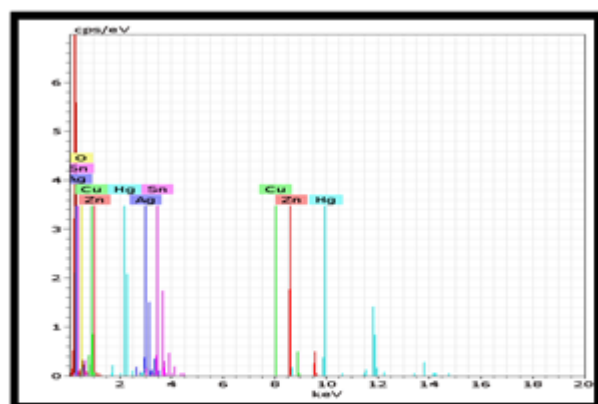


Figure f Shows spectrum of EDS analysis for the second region of amalgam B.

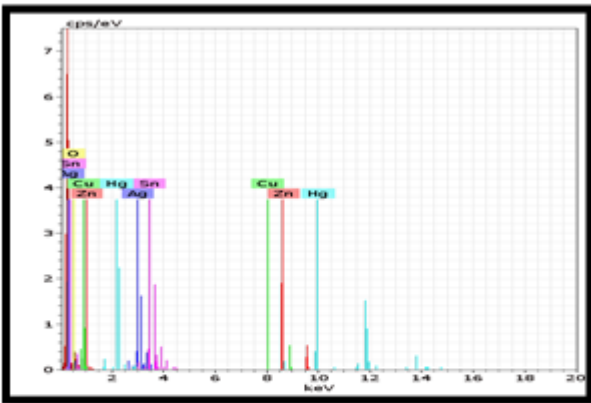


Figure g Shows spectrum of EDS analysis for the third region of amalgam B.

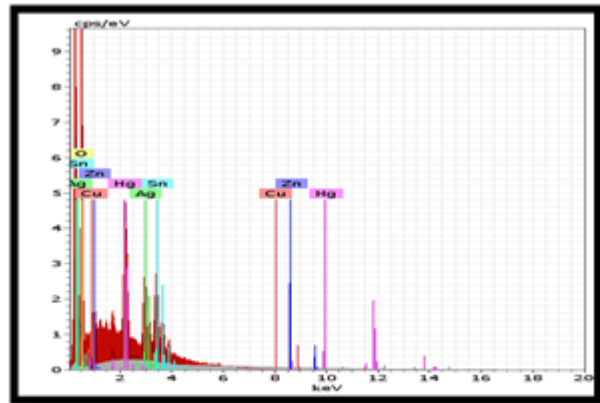


Figure h Shows spectrum of EDS analysis for the fourth region of amalgam B.

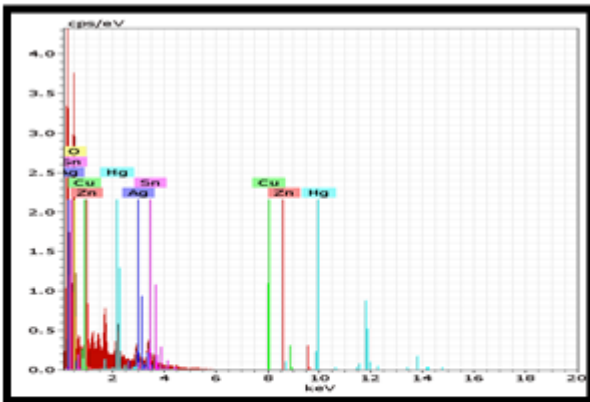


Figure i Shows spectrum of EDS analysis for the first region of amalgam C.

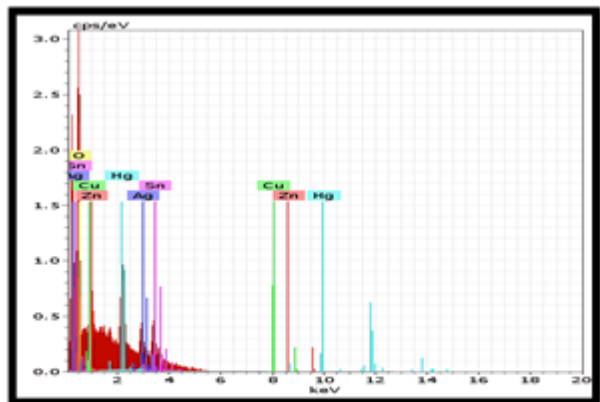


Figure j Shows spectrum of EDS analysis for the second region of amalgam C.

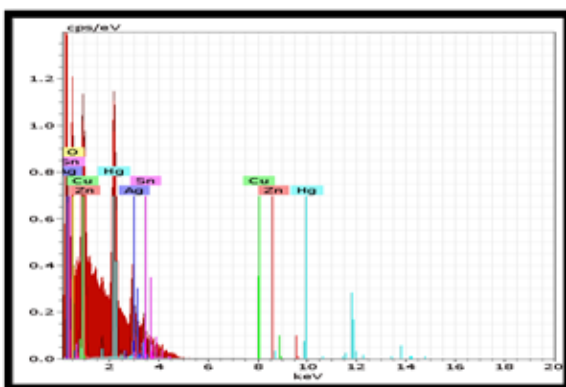


Figure k Shows spectrum of EDS analysis for the third region of amalgam C.

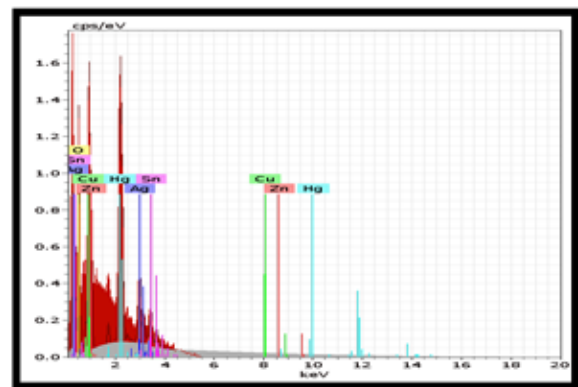


Figure m Shows spectrum of EDS analysis for the fourth region of amalgam C.

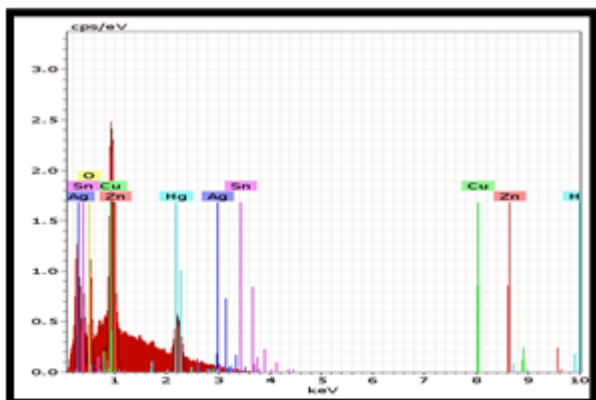


Figure n Shows spectrum of EDS analysis for the first region of amalgam D.

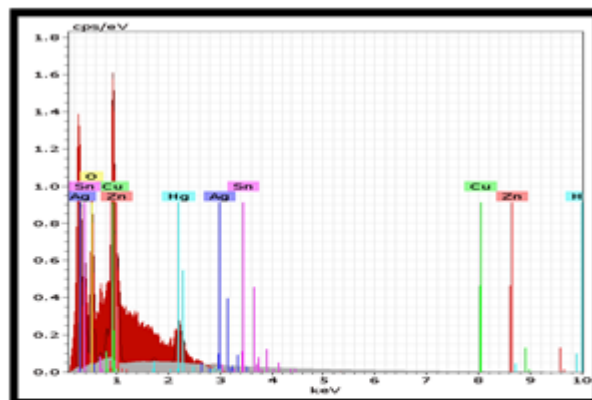


Figure o Shows spectrum of EDS analysis for the second region of amalgam D.

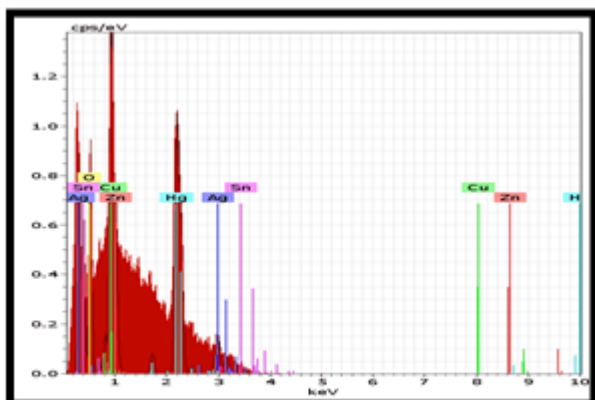


Figure p Shows spectrum of EDS analysis for the third region of amalgam D.

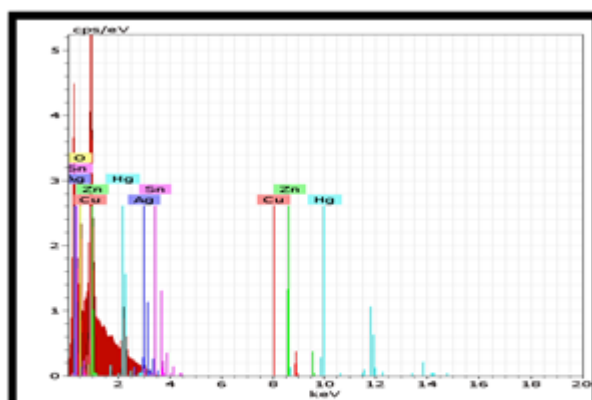


Figure q Shows spectrum of EDS analysis for the first region of amalgam E.

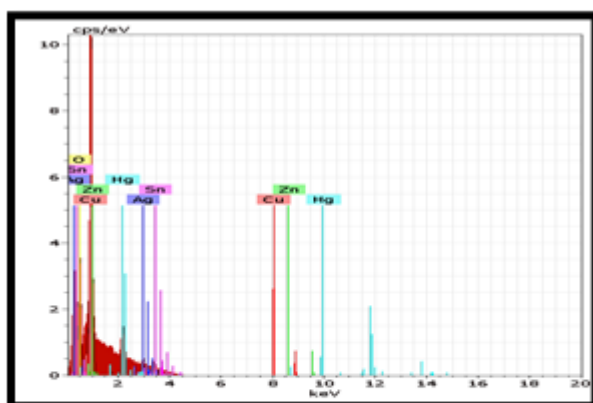


Figure r Shows spectrum of EDS analysis for the second region of amalgam E.

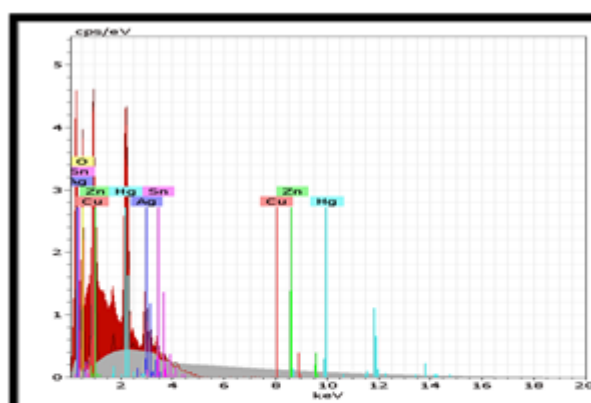


Figure s Shows spectrum of EDS analysis for the third region of amalgam E.

The OCP – time was measured in reference to SCE in synthetic saliva at 37 ± 1 C° for all tested amalgams. **Figure 9** shows the evolution of corrosion potential of the amalgams

throughout time. The time period goes upto 135 minutes and with interval of five minutes were potential reported. The mean value of the OCP were recorded by using two specimens for each amalgam.

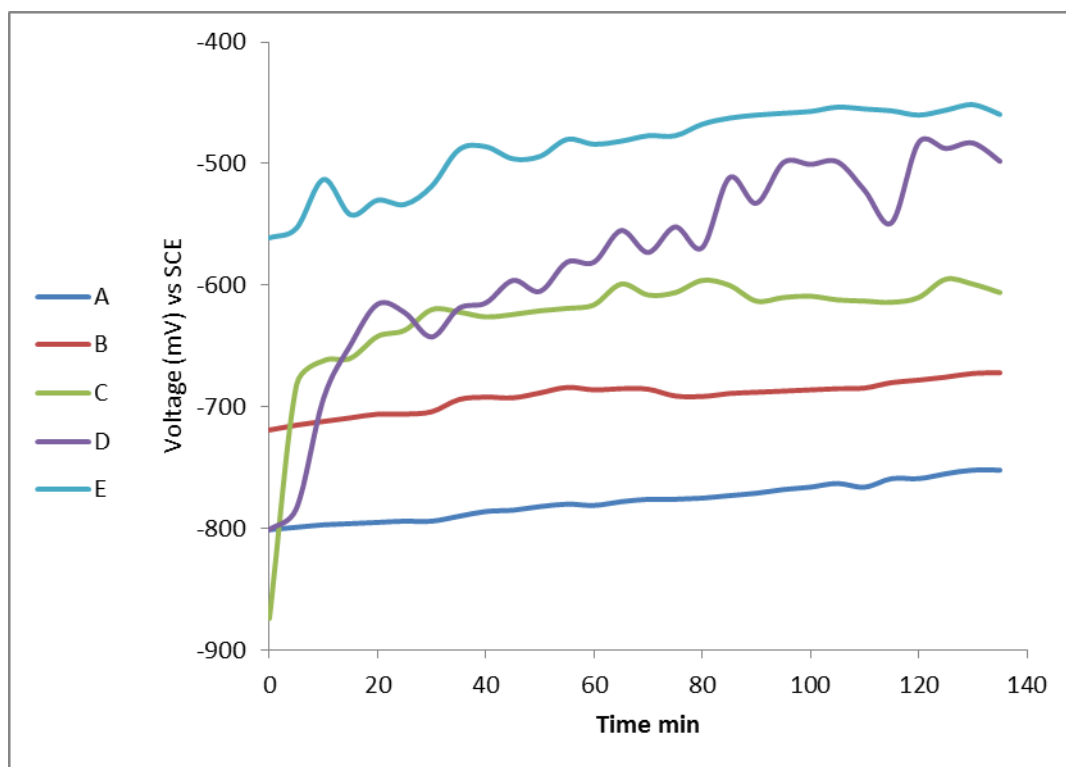


Figure 9 Shows the OCP-time of amalgams.

Figure 9 shows the variation of open circuit potential (OCP) with time from which several deductions can be made. The first is that during the first 30 minutes were studied the corrosion potential increases at a greatest speed in this period in every case study. This initial increasing generally seems to be related to the formation and thickening of the oxide film on the surface, increases its corrosion protection ability. Afterwards, the OCP increases slowly because of the growth of the film onto the metallic surface.

The second is that the corrosion potential reach a level from which corrosion potential tends to stabilize. The constant OCP means that there is equilibrium between dissolution and deposition.

From Figure 9, it is obvious that the addition of copper increases the corrosion resistance (increase nobility). This is because the decrease of γ_2 which is the weakest phase against corrosion and the

increases in η phase which is more corrosion resistance than γ_2 .

The polarisation curves are shown in Figure 10 recorded after 30 min immersion, and data from these curves (the related corrosion current densities, corrosion potentials and the calculated corrosion rate) are summarized in Table 3. It should be observed that the corrosion potentials are more negative than the open circuit values, which can be attributed to the potentials used that reduce the thickness of the oxide film.

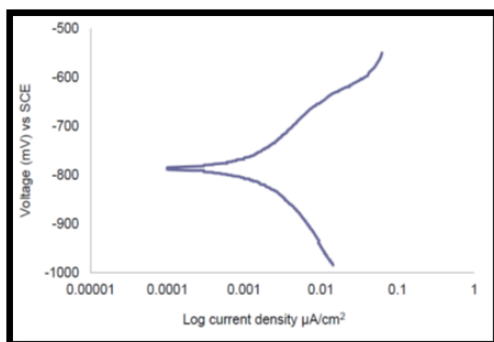
These results demonstrate that the corrosion behavior of the studied dental amalgam alloys varied according to the composition of the alloys in which the results showed a reduction in the average corrosion current densities values of amalgams with increasing copper content and, hence, increasing corrosion resistance with increasing copper content.

Table 3 illustrates the corrosion potential (E_{corr}), corrosion current density (i_{corr}) and corrosion rate.

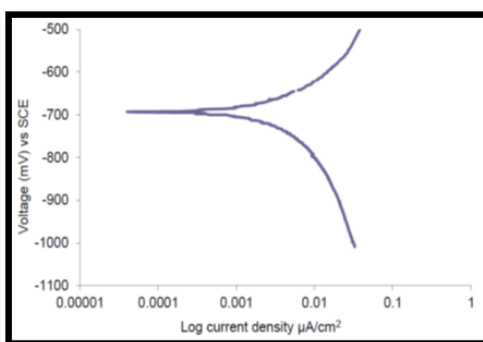
Alloy	Mean E_{corr} (mV)	$i_{\text{corr}} * 10^{-6}$ (mA/cm ²)	Corrosion Rate (mpy)
A	-786	946.4	0.727
B	-692	795.81	0.617
C	-614	768	0.602
D	-600	751	0.595
E	-420	484	0.388

The lower resistance to corrosion of the low-copper amalgam is attributed to the presence of the γ_2 phase within amalgam microstructure which is the most anodic phase of the present phases of the set

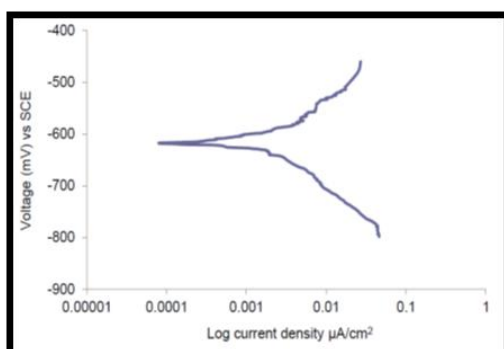
amalgam and the most the corrosion-prone one. On the other hand, the high-copper amalgam formed a tin-copper phase (η phase) in large quantities and minimum amount of the γ_2 phase.



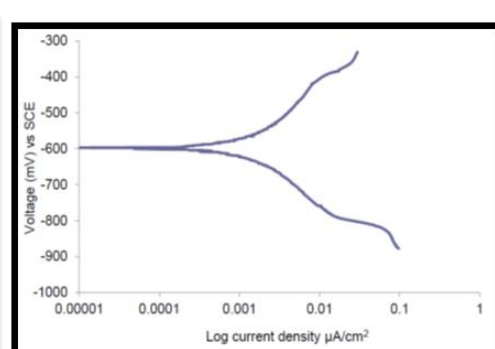
Amalgam (a)



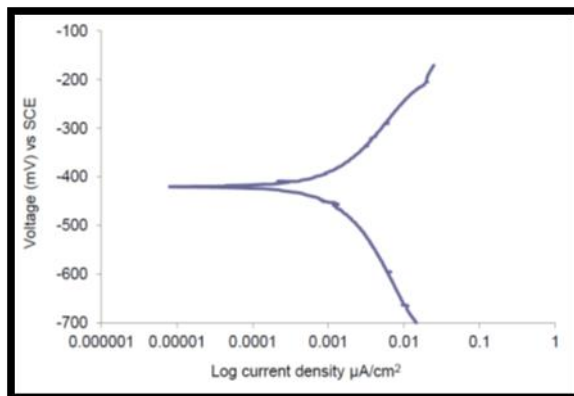
Amalgam (b)



Amalgam (c)



Amalgam (d)



Amalgam (e)

Figure10 Thepotiodinamicpolarization curve amalgams.

4.CONCLUSION

- 1- The presence of copper in high percentages leads to the creation of the tin-copper phase and reduces the chance for the formation of the corrosion-susceptible tin-mercury phase, which thus helps improve the amalgam's resistance to corrosion.
- 2- Open circuit potential measurements curves present corrosion potentials most positive for high copper dental amalgam reflecting the order of corrosion resistance.
- 3- Increasing copper content improve corrosion resistance of dental amalgam by 46 % compared to low copper dental amalgam.

5.REFERENCES

1. R. Bharti, "Dental amalgam: An update," Journal Of Conservative Dentistry, vol. 13, no. 4, pp. 204-208, 2010.
2. J. R. Davis, *Metals Handbook Desk Edition*, 2nd ed. USA: ASM, 1998.
3. S. Aditya et. al. "Assessment of mercury release from dental amalgam: an in vitro study," International Research Journal Of Pharmacy, vol. 4, no. 8, pp. 237-239, 2013.
4. Haydar H. Jamal Al-deen and Nabaa Muthana Mahdi, Effect of (ZrO₂) Addition on Mechanical and Electrochemical Properties and Thermal Conductivity of High Copper Dental Amalgam" Advances In Natural And Applied Sciences, Vol. 11, No. 1, pp. 66 – 76, 2017.
5. Y. Uc, ar and W. A. Brantley, "Biocompatibility of Dental Amalgams," International Journal of Dentistry, pp. 1-7, 2011.
6. .W. Osborne, J.B. Summitt and H.W. Roberts, "The use of dental amalgam in pediatric dentistry: review of the literature", Journal of Pediatric Dentistry, vol. 24, no.5, pp. 439- 447, 2002.
7. B.W. Darvell, "Effect Of Corrosion On The Strength Of Dental Silver Amalgam," Journal Of Dental Materials, vol. 28, no.1, pp. 160-167, 2012.
8. R. G. Craig and J. M.Powers, *Restorative dental materials*, 11th ed. USA: Mosby, 2002.
9. S. H. Soratur, *Essentials Of Dental Materials*, New Delhi: Jaypee Brothers Medical Publishers, 2007.
10. C. M. Brett and F. Trandafir, "The corrosion of dental amalgam in artificial salivas: an electrochemical impedance study," Journal of Electroanalytical Chemistry, Vol.572, no.1, pp. 347–354, 2004.
11. M. Fathi, and V. Mortazavi, " Comparative Evaluation of The Initial Corrosion of Four Brand of High Copper Dental Amalgam," Journal of Dentistry Research in Medical Sciences, vol. 1, no. 3, pp. 48-55, 2004.
12. H. A. Acciari et al. "Corrosion of dental amalgams: electrochemical study of Ag–Hg,

- Ag–Sn and Sn–Hg phases,” *Electrochimica Acta*, vol. 46, no.1, pp. 3887–3893, 2001.
13. R. A. Majed et al. “*Experimental Study and Mathematical Modeling for Corrosion of Amalgam at Different Periods*,” *Tikrit Journal for Dental Sciences*, vol.1, no.1, pp. 30-37, 2013.
 14. Haydar H. Jamal Al-deen and Sura Ali Shahee “Replacement Of Mercury With Gallium Alloy In Dental Fills” *International Journal of Scientific & Engineering Research*, Vol. 6, no. 12, pp. 2229 – 5518, 2015.
 15. *Guide to Dental Materials and Devices*, 7th edition, (A.D.A.), 1974-1975.
 16. F. C. Allan, K. Asgar, and F. A. Peyton, “*Microstructure of Dental Amalgam*,” *Journal Of Dental Research*, vol.44, no.5, pp. 1003-1012, 1965.
 17. W. M. Amin, “*Comparative Electrochemical Investigation of The Effect of Aging on Corrosion of Dental Amalgam*,” *Quintessence International*, vol. 38, no. 7, pp. 417-424, 2007.
 18. *Annual Book of ASTM Standards, Wear and erosion; Metal Corrosion*, volume 03.02, G5 – 87, 1988.
 19. Fontana and Green, *Corrosion Engineering*, McGraw – Hill Book Company, 1978.
 20. Rasha Safaa Hadi, Haydar H. Jamal Al-deen and Nabaa S. Radhi “Investigation the Coating of Hydroxyapatite on Titanium Substrate by Pulse Laser Deposition” *Journal of University of Babylon for Engineering Sciences*, Vol. 26, No. 10, pp. 299 – 311, 2018.